



## Research paper

# Bridge headwater afflux estimation using bootstrap resampling method

Marta Kiraga<sup>1</sup>, Sławomir Bajkowski<sup>2</sup>, Janusz Urbański<sup>3</sup>

**Abstract:** The bridge structure's development causes a riverbed cross-sections contraction. This influences the flow regime, being visible during catastrophic floods. Then the flow velocity increases and water piles up upstream the bridge, where headwater afflux could be observed. These changes depend on the watercourse geometry and the bridge cross-section properties, especially on the degree of flow contraction under the bridge. Hydraulic conditions under the bridge depend on flow velocity, dimensions, and shape of abutments, the granulometric composition of bedload, which can be quantitatively characterized by hydraulic resistance coefficients. The research subject of headwater afflux is equated with the recognition of morphodynamic processes occurring along the passage route. The headwater afflux could be estimated by empirical formulas and by the energy method using Bernoulli's law. Empirical methods are optimized by adopting various statistical criteria. This paper compares the headwater afflux values calculated using two existing empirical formulas, Rehbock and Yarnell, and compares them with the results of laboratory tests. Following the assumption that the free water surface is influenced by flow resistance, an attempt was made to include friction velocity in the empirical formulas. Based on the Authors' database, the coefficients used were optimized using bootstrap resampling in Monte Carlo simulation. The analyses demonstrated that the formula best describing the phenomenon of headwater afflux upstream the bridge is an empirical formula built based on the historical Yarnell formula, which includes friction velocity value. The optimized equation provides an average relative error of 12.9% in relation to laboratory observations.

**Keywords:** local scour, sediment, hydraulic structures, hydraulics, flood, bridge engineering

<sup>1</sup>DSc., PhD., Eng., Warsaw University of Life Sciences, Institute of Civil Engineering, Faculty of Civil and Environmental Engineering, ul. Nowoursynowska 159, 02-776 Warsaw, Poland, e-mail: [marta\\_kiraga@sggw.edu.pl](mailto:marta_kiraga@sggw.edu.pl), ORCID: 0000-0001-9729-4209

<sup>2</sup>Prof., DSc., PhD., Eng., Warsaw University of Life Sciences, Institute of Civil Engineering, Faculty of Civil and Environmental Engineering, ul. Nowoursynowska 159, 02-776 Warsaw, Poland, e-mail: [slawomir\\_bajkowski@sggw.edu.pl](mailto:slawomir_bajkowski@sggw.edu.pl), ORCID: 0000-0002-7010-0600

<sup>3</sup>DSc., PhD., Eng., Warsaw University of Life Sciences, Institute of Civil Engineering, Faculty of Civil and Environmental Engineering, ul. Nowoursynowska 159, 02-776 Warsaw, Poland, e-mail: [janusz\\_urbancki@sggw.edu.pl](mailto:janusz_urbancki@sggw.edu.pl), ORCID: 0000-0001-7689-3667

## 1. Introduction

Piers connect the bridge superstructure to the substrate through foundations located in riverbeds or floodplains. Hydraulic calculations of bridges include minimum bridge span determination, estimation of the expected channel deepening at the bridge cross-section, calculation of the water surface elevation upstream the bridge, and prediction of local scour at the pier region [1–3]. During flood periods, the water level and the flow velocity increase, and velocities distribution is varied. On the inflow side, the subsurface stream flows upward toward the free water surface upstream of the pier head, while the bottom stream is diverted to the riverbed (Fig. 1). Masses of water flow around the pier (1 in Fig. 1) – upward-directed masses induce a frontal wave upstream the pier (2 in Fig. 1). The stream hitting the bottom causes the horseshoe vortices formation (3 in Fig. 1) [4,5]. Initial vortices are formed, eventually taking the form of a lee-wake vortice (4 in Fig. 1). Vertical vortices passing downstream generate a runoff vortex zone with farwater vortices occurring downstream the bridge cross-section (5 in Fig. 1). The deformation of velocity pattern and the increase of bottom velocities cause the development of a scour hole around the pier (6 in Fig. 1). The bridge pier constructional design affects the cross-section of the watercourse narrowing in relation to undisturbed flow conditions (7 on Fig. 1) and causes afflux formation upstream of the bridge (8 on Fig. 1). The height of the headwater afflux is affected by increasing flow resistance along with the pier structure. These resistances depend on the watercourse geometry properties, the shape of the bridge cross-section, the channel narrowing and widening degree, the flow velocity, and the type, shape, and dimensions of the bridge abutments.

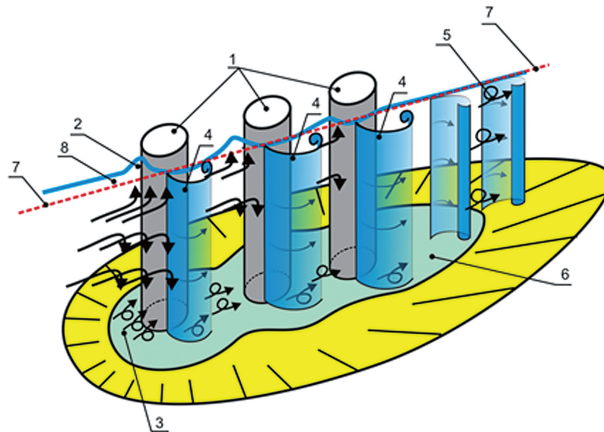


Fig. 1. Flow pattern and local scour around a cylindrical pier schematic: 1 – column pier, 2 – bow wave, 3 – horseshoe vortice, 4 – lee-wake vortice, 5 – farwater vortice, 6 – local scouring area, 7 – water surface level without the structure introduction; 8 – headwater afflux upstream the pier

Three stages of the scouring process can be distinguished: the initial stage related to the scouring initiation, the proper stage, which is the period of scour development

and deepening, and the final stage, in which the shape stabilization could be observed. The most significant initial stage could be pointed to, which is characterized by the high stream velocities occurrence in the bottom region and high stream turbulence [4–8]. The water surface elevation along the river reach depends not only on the hydraulic structure properties but also on the local granulometric conditions, which can be quantitatively characterized by hydraulic resistance coefficients. Hydraulic resistance could be described using empirical coefficients or shear stresses on the wetted channel perimeter, expressed as friction velocity.

The study of headwater afflux was initiated in the late 19th century by D'Aubuisson, whose formula based on hydraulic conditions was verified by Weisbach in 1848 and Rühlmann in 1880 [9]. In the early 20th century, Nagler and Lane verified D'Aubuisson's formula using their experimental data and modified Weisbach's formula [9]. Thereafter, Rehbock and Yarnell conducted a large number of laboratory experiments, continuing the earlier studies of the bridge afflux phenomenon. In addition to the Rehbock, Yarnell, Nagler, and D'Aubuisson formulas, the USBR equation is used. The small number of research approaches indicates that verification of estimation results is difficult due to the local range of data and studies [10]. Liang et al. (2020) [10] cite 30 experiments by various authors that resulted in equation formulation for estimating the geometric parameters of local scour, whereas there are only 10 formulas in practical for determining the magnitude of afflux upstream the bridge piers.

The present paper compares the headwater afflux estimating results using two of the best-known empirical formulas: the Rehbock and the Yarnell method. These methods use coefficients determined from laboratory tests conducted for various structural solutions of the piers. The formula coefficients were optimized using bootstrap resampling in Monte Carlo simulation based on the authors' database. Following the assumption that the channel morphodynamic properties also influence the water surface structure in the pier region, the possibility of dynamic velocity including in the empirical formulae for afflux estimating was examined.

## 2. Materials and methods

### 2.1. Laboratory experiments

The physical model studies of the afflux phenomenon on the bridge pier were carried out in the Hydraulic Laboratory of the Warsaw University of Life Sciences WULS. 19 experimental series were performed, each lasted 8 h. Studies were conducted in a flume with a rectangular cross-section, width  $B = 0.58$  m, filled with alluvial sand with a medium diameter of  $d_{50} = 0.91$  mm over a length of 8.00 meters of working section. The soil grain size curve is shown in Fig. 2. To eliminate changes in grain size characteristics as a result of repeated measurements in different research variants, two soil samples each were taken before and after the experiments. Samples "1" and "2" were taken from the deeper layer of the subsoil, while samples "3" and "4" were taken from the bottom surface. No significant

changes in the grain size of the samples were observed during the tests, which is confirmed by the course of the sieving curves shown in Figure 2. Sand layer was equal to 25 cm in the region of piers.

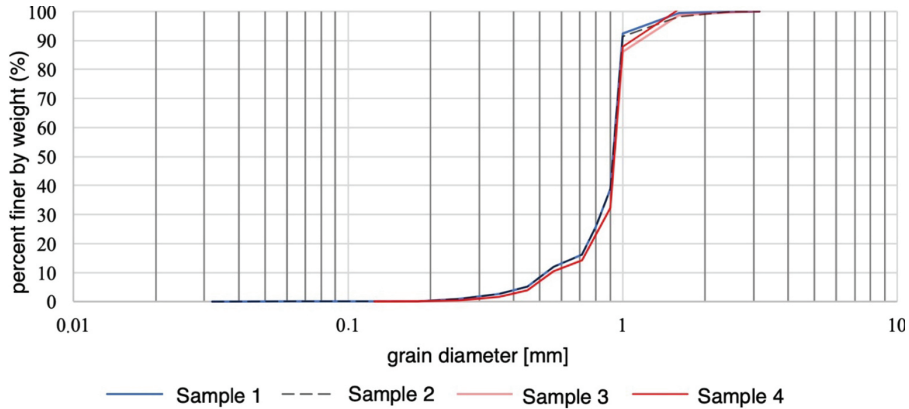


Fig. 2. Grain size curve of the bottom material

The bottom material is coarse sand, uniformly grained and well sorted. The degree of soil compaction was tested in each measurement series directly before introducing water into the flume. The degree of compaction  $I_D$  was between 0.77 and 0.82, which means the soil was in compacted form. Prior to each measurement, the sand was compacted in a standardized manner with a 3.5 kg hand compactor lowered to the bottom surface with an energy of about 5 J.

The bridge pier model consists of three piles of circular cross-sections with diameters  $D = 0.05$  m (Fig. 3a, b, c). For this type of pier structure, the equivalent width of the group pillar was  $w = D = 0.05$  m, and the equivalent length was  $m = 0.20$  m, resulting in a ratio  $w/m = 0.25$ . The local scouring phenomenon and the water surface shape evolution in the bridge pier area were observed. Measurements were made using a movable pin gauge installed on guides along the flume. Measurement readings were taken at cross-sections located from each other at intervals of 0.01 to 0.07 m. In the pier model area, the measurement grid was concentrated to  $(1 \times 5)$  cm and  $(5 \times 7)$  cm (Fig. 4a). The experiment was performed in the steady flow conditions within a discharge range of  $Q_w = 0.030$ – $0.040$   $\text{m}^3 \cdot \text{s}^{-1}$ . The conceptual scheme is demonstrated in Figure 4b. Bernoulli's equation for cross-sections 1 and 3, upstream and downstream the bridge could be written followingly:

$$(2.1) \quad h_1 + \frac{\alpha v_1^2}{2g} = h_3 + \frac{\alpha v_3^2}{2g} + \Delta H_{1-3}$$

where:  $h_1, h_3$  – water depth upstream and downstream the pier [m],  $v_1, v_3$  – average water velocity upstream and downstream of the pier [ $\text{m} \cdot \text{s}^{-1}$ ],  $\Delta H_{1-3}$  – energy gradient.

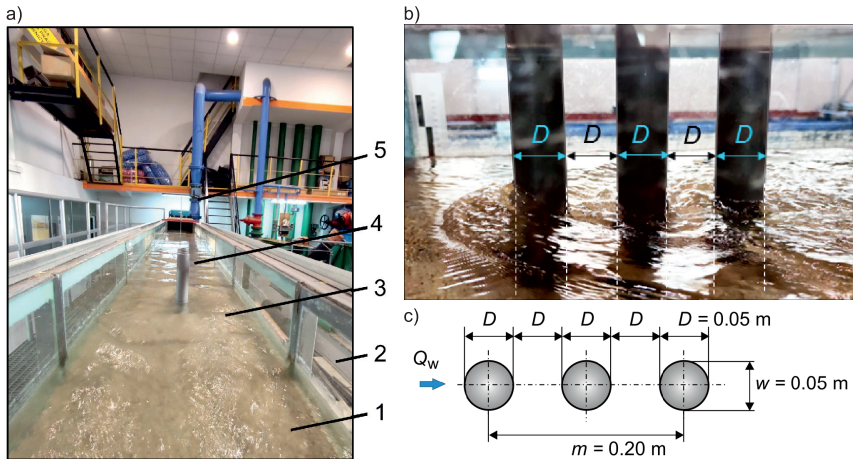


Fig. 3. Laboratory model; a) the view from downstream, 1 – tilting flume, 2 – glass wall, 3 – alluvial bed, 4 – bridge pier model, 5 – water-conducting pipeline; b) pier model profile,  $D$  – pier diameter,  $m$  – equivalent length of the pier wall,  $w$  – group pier width; c) laboratory pier model cross-section

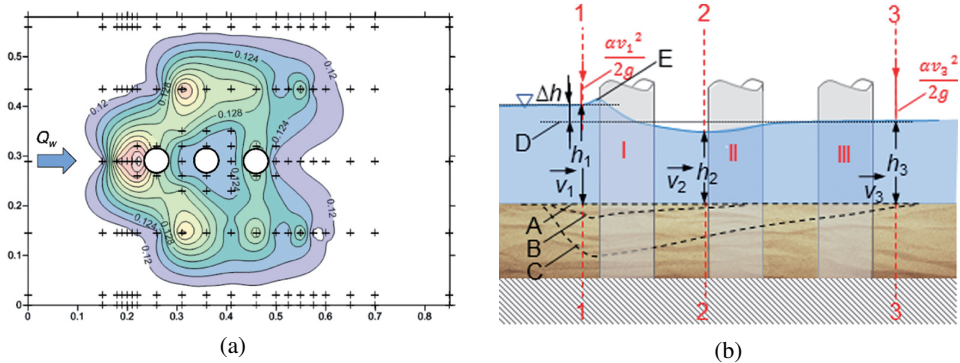


Fig. 4. Schematic diagrams of research, a) measurement grid with isolines for water discharge  $Q_w = 0.0399 \text{ m}^3 \cdot \text{s}^{-1}$ , water depth in control profile  $h_0 = 0.1205 \text{ m}$ ; b) side view, where: I, II, III – pile pier numbers, A – bed shape before structure introduction, B – the initial stage of local scouring, C – well-shaped scour, D – water surface before structure introduction, E – bow wave;  $h_1, h_2, h_3$  – water depths: upstream, along the pier, downstream, [m],  $v_1, v_2, v_3$  – water velocity: upstream, along the pier, downstream, [ $\text{m} \cdot \text{s}^{-1}$ ],  $\Delta h$  – the headwater afflux, [m]

## 2.2. Empirical formulas

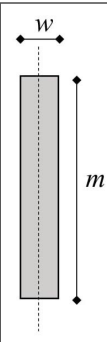
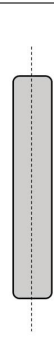



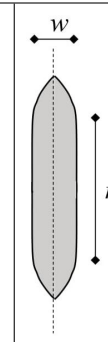
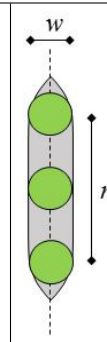


The empirical methods for headwater afflux height estimation developed by Rehbock [12] and Yarnell [13] consider parameters that characterize the pier geometry and constant values of coefficients. The Rehbock formula has the general form:

$$(2.2) \quad \Delta h = \delta(a + b\alpha_0 + c\alpha_0^4) (1 + 2\omega) \alpha_0 \frac{v_3^2}{2g}$$

where:  $\delta$  – coefficient characterizing the pier geometry, selected from the literature [14], given in Table 1,  $a = 0.72$ ,  $b = 1.20$ ,  $c = 40.0$  – dimensionless coefficients, which are subject of verification and optimization in this research approach,  $\alpha_0$  – the ratio of upstream pier face inflow area to the total flow area in the cross-section downstream the bridge,  $\omega$  – the ratio of the velocity head to the water depth in the cross-section downstream the bridge,  $v_3$  – average water velocity downstream the pier [ $\text{m}\cdot\text{s}^{-1}$ ].

The geometry of the three-pile cylindrical pier was described by a coefficient  $\delta$  equal to 1.65, determined by the ratio  $(w/m) = 0.25$  (Figure 4b), the same as for a solid pier with circular lower and upper head. An extended set of coefficients, describing a given pier geometry structure, was developed based on the approach of Kubrak and Nachlik (2003) [14], considering a three-pile pier with no junction between the piles (Table 1). The Rehbock and Yarnell formulas were chosen because of their relatively simple form, with variables whose components could be directly measured in the laboratory. In addition, it was easy to extract dimensionless function parameters that could be subjected to a Monte Carlo sampling procedure.

Table 1. An extended summary of shape coefficients  $\delta$  for the Rehbock's (extended approach based on Kubrak and Nachlik 2003 [14], including multipile piers)

Pier type									
$w$ [m]	3.00	3.00	3.00	3.00	3.00	3.00	0.05	3.00	3.00
$m$ [m]	20.00	19.25	18.50	17.00	15.00	12.06	0.20	8.90	2.00
$\delta$ [-]	3.90	2.87	2.42	2.10	1.84	1.65		1.45	1.06
$(w/m)$	0.15	0.156	0.162	0.18	0.20	0.25	0.25	0.34	1.50
Chosen for present pier construction:						0.25			


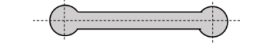

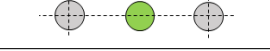
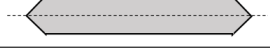
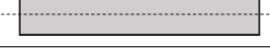
Yarnell formula has the following general form:

$$(2.3) \quad \Delta h = 2K(K + 10\omega - 0.6) \left( d\alpha_0 + k\alpha_0^4 \right) \frac{v_3^2}{2g}$$

where:  $K$  – a friction factor, dependent on pier shape in plan, taken from the Table 2,  $\omega$  – the ratio of the velocity head to the water depth in the cross-section downstream the bridge,  $d = 1.00$ ,  $k = 15.00$  – dimensionless coefficients, which are subject of verification and

optimization in this research approach. The friction factor  $K$  was taken to be equal to 1.05, the same as Tyimiński (2010) [15] takes for a two-pile pier with no junction. Table 2 is an extension of the parameter values compiled by Tyimiński [15].

Table 2. Shape coefficients  $K$  for Yarnell's formula (an extended approach based on Tyimiński 2010 [15], including multiple piers)

Pier type		$K$ [-]
Semi-circular edge		0.90
Two-column pier with junction wall		0.95
Two-column pier without junction wall		1.05
Three-column pier without junction wall		
Sharp-crested edge		1.05
Rectangular		1.25

### 2.3. Friction velocity estimation

Friction velocity is a quantity used to description of sediment transport processes and the structure of the turbulent flow. The friction velocity  $v_*$  can be estimated as:

$$(2.4) \quad v_* = \sqrt{gR_{hb}I}$$

where:  $R_{hb}$  is hydraulic radius referred to the bottom, [m], and  $I$  is energy level gradient, [-].

Hydraulic radius referred to the bottom could be estimated based on Einstein's hypothesis (1950) [16], which assumes the whole cross-section area division into specific fields, where flow resistance is explicitly diversified and related to various roughness of bed and bank material (or glass panel, in the laboratory flume). This method is predicated on the assumption that in distinguished parts of the flume (Fig. 5) average stream velocity  $v_s$  – in the glass panel impact zone with  $A_s$  area and  $v_b$  – in the bottom impact zone with  $A_b$  area, is equal to average stream velocity  $v$  in the whole cross-section:

$$(2.5) \quad v = v_s = v_b$$

Expressing the average velocity by the Darcy–Weisbach formula, the equation can be given:

$$(2.6) \quad \frac{1}{\sqrt{\lambda_t}} \sqrt{8gR_{ht}I} = \frac{1}{\sqrt{\lambda_s}} \sqrt{8gR_{hs}I} = \frac{1}{\sqrt{\lambda_b}} \sqrt{8gR_{hb}I}$$

where:  $\lambda_t$ ,  $\lambda_s$ ,  $\lambda_b$  – the hydraulic resistance coefficient: total, for the side-wall, for the bottom, [-];  $R_{ht}$ ,  $R_{hs}$ ,  $R_{hb}$  – the hydraulic radius: total, of the flow area part connected with the side-wall roughness [m]; of the flow area part connected with the bottom roughness.

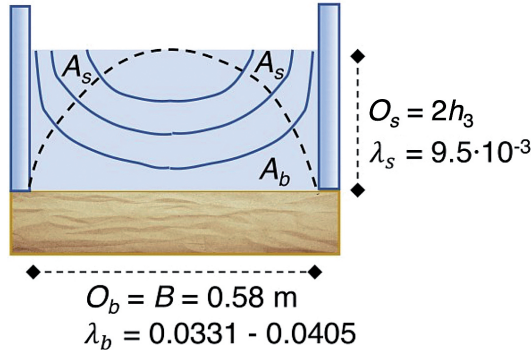


Fig. 5. Velocity field distribution scheme within the cross-section according to Einstein hypothesis, where:  $A_s$  – the velocity field area within the glass panel impact zone with  $O_s$  wetted perimeter and  $\lambda_s$  hydraulic resistance coefficient;  $A_b$  – the velocity field area within the bottom impact zone with  $O_b$  wetted perimeter and  $\lambda_b$  hydraulic resistance coefficient

The velocity distribution depends on the interrelationship between the values of the hydraulic resistance coefficients for the whole cross-section  $\lambda_t$ , for the panels  $\lambda_s$  and the bottom of the flume  $\lambda_b$ . Following the study of Urbanski (2009) [17],  $\lambda_s = 9.5 \cdot 10^{-3}$  was assumed for the glass panels. Based on the average stream velocity in the cross-section  $v_0$  known in each measurement series, the value of  $\lambda_t$  was calculated using the transformed Darcy–Weisbach formula and subsequently using the following relation:

$$(2.7) \quad \lambda_t = \frac{\sum \lambda_i O_i}{\sum O_i}$$

the value of the bottom resistance coefficient was calculated  $\lambda_b$  for known partial perimeter lengths  $O_i$ :  $O_s = 2h_3$  for glass panels;  $O_b = B = 0.58$  m for the bottom.

Unknown hydraulic resistance coefficient values  $R_{hs}$  and  $R_{hb}$  were estimated using an iterative procedure based on  $R_{hs}$  and  $R_{hb}$  values selection, as to respect the following relations between them (Kubrak and Nachlik 2003), [14]:

$$(2.8) \quad R_{ht} = \frac{A_t}{O_t}, \quad R_{hs} = \frac{A_s}{O_s}, \quad R_{hb} = \frac{A_b}{O_b}$$

and the total flow area was equal to:

$$(2.9) \quad A_t = 2A_s + A_b$$

Hydraulic radiuses and resistance coefficients for each separate part of the cross-section were estimated from iterative calculations according to the Colebrook-White equation:

$$(2.10) \quad \frac{1}{\sqrt{\lambda_t}} = -2 \log \left( \frac{2.51}{\text{Re} \sqrt{\lambda_t}} + \frac{k_s/d}{3.71} \right)$$



where:  $k_s$  – absolute cross-section roughness, for the velocity field connected with the bottom  $k_{s,b} = 3d_{90} = 0.0045$  m [18] and with glass walls  $k_{s,g} = 3.0 \cdot 10^{-6}$  m [19] and  $Re$  – Reynold's number.

The procedure of formulas optimization assumes the preparation of dimensionless coefficients value ranges. The samples of coefficient values sets are randomized using a quasi-random generator within the established ranges. To take advantage of the generated test ranges, an additional conversion factor of 10 was introduced, due to the order of magnitude of friction velocity and downstream jet velocity observed during laboratory tests. Accordingly, the modified forms were obtained:

– of Rehbock's formula

$$(2.11) \quad \Delta h = \delta(a + b\alpha_0 + c\alpha_0^4) (1 + 2\omega) \alpha_0 \frac{(10v_*)^2}{2g}$$

– and Yarnell's formula

$$(2.12) \quad \Delta h = 2K(K + 10\omega - 0.6) \left( d\alpha_0 + k\alpha_0^4 \right) \frac{(10v_*)^2}{2g}$$

## 2.4. Formulas optimization

Computational support of analytical and operational processes in the hydraulic engineering field requires the use of technologies and tools of substantial diversity. For some problems, algorithmic solutions (using appropriate mathematical models) are used, while others require a heuristic approach (based on artificial intelligence methods and tools) [20, 21]. The objective of the used procedure was to obtain optimized equations forms, describing the results of laboratory measurements. The Monte Carlo method allows adjusting the values of dimensionless coefficients of the calculation formulas so that they describe the observed phenomenon as closely as possible – in this case, so that the calculated afflux is as close as possible to the observed one. The measure of the formulas accuracy was the average relative error of the calculations to the observations for all 19 measurement series – the smaller, the more precisely the function describes the laboratory results. The procedure involves repeatedly sampling random numbers within an assumed range of values and calculating the average error for all measurement series using an equation described by a given set of parameters. The preliminary, trial, and archival measurements that are not part of the database used in this study, but performed under the same granulometric and hydraulic conditions provided some historical database that was used for bootstrap resampling.

Bootstrap methods have been known for more than 30 years; however, they have only recently begun to be widely used in stochastic simulation models. The basis of the bootstrap method is the assumption that the future is similar to the past. Instead of studying the past and attempting to describe it using theoretical distributions and then simulating the future using the chosen distributions, input to the simulation can be generated directly from historical data [22, 23]. Bootstrap resampling is a method that involves randomization of sample data repeatedly with replacement from a data source to estimate a parameter population.

In the Monte Carlo sampling method, one complete simulation experiment indicates performing  $n$  repetitions on randomly generated input values [22]. Before each simulation repetition, values are randomized from a sample of historical data (jackknifing). Each repetition is therefore executed on a different random sample. The value once taken returns back again to the historical sample. Therefore, the base of the procedure is sampling with replacement, which means that in each bootstrap sample some historical data may occur many times and some will not be represented at all.

Multi-parameter empirical equations with unspecified individual parameters values ranges are usually developed for a given group of objects or conditions – and this is the limit of their applicability. In order to extend it, a given formula should be verified on a new site – by means of physical or mathematical modeling or field testing. The verification of an empirical formula with its original dimensionless coefficients does not always give reliable results – and changing the coefficients value provides an approximation of the directly measured results to the calculated data. Hence the necessity arises to determine the optimal parameters of the investigated function. The criterion for the selection may be based on statistical measures, but in the case of verification of functions describing quantities that can be measured directly in the laboratory, the criterion of the smallest average relative error seems to be appropriate.

The historical database was constructed from 10 series of partial, pilot measurements taken for teaching purposes. Thus, 10 headwater afflux values were obtained for various hydraulic conditions. For verification of Rehbock and Yarnell formulae, 10.000 combinations of dimensionless parameters of the tested formulae were selected for each function. Also, each function coefficient was assumed to be sampled within  $\pm 50\%$  of the initial coefficient value. The combinations were generated using a random number generator. Guided by the mean relative error criterion, combinations of function parameters describing well the laboratory results were selected. In their case the average relative error was  $< 35\%$ . There was  $k$  such combinations, and the parameters assigned to them had indexes  $1 - k$ , where  $k = 300$  (Fig. 6).

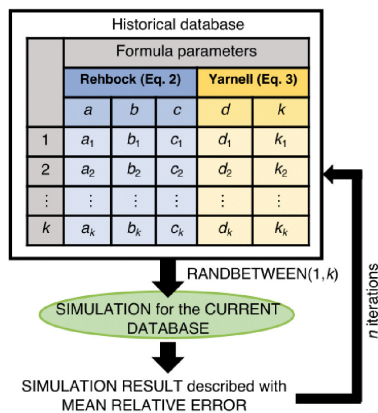


Fig. 6. Bootstrap resampling schematic diagram on the example of resampling equation (2.2) and (2.3)

The  $\text{RANDBETWEEN}(1/k)$  formula was subsequently used to randomly determine the value index used in the current iteration. For a sampled set of coefficients values, calculations were performed for a database (CURRENT DATABASE) consisting of 19 measurement series with the full range of measurements to be performed and the full duration of the measurement series, described in Table 3 in Results part of the present publication, and the average relative error of the formula against the measurements was calculated. The  $1 - k$  index randomization was performed  $n$  times, where  $n = 10.000$ .

### 3. Results

Table 3 provides a summary of parameters characterizing the hydraulic conditions of the measurements. The headwater afflux was measured within the range of 0.0094–0.0187 m, which constitutes 1.6–10.4% of water height in control profile 0–0, located 1.00 m upstream the model. The free water surface was transformed into graphical form according to the measurement points distribution shown in Figure 4a. Spatial representation of the water surface in the three-dimensional form is shown in Figure 7. A point cloud describing the water surface spatial distribution was entered into Meshlab software, where the mesh was generated, creating a bow wave, the headwater afflux, and the local collapse of the water surface. The Froude number in each case indicated subcritical flow ( $Fr < 1$ ).

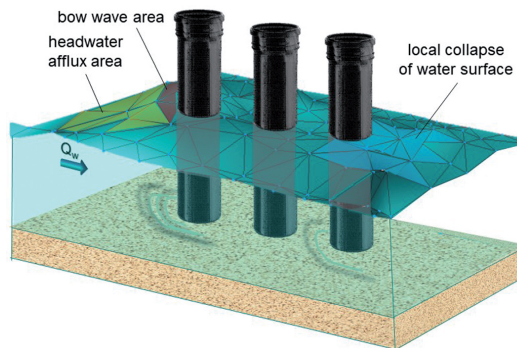


Fig. 7. Graphical representation of the water surface in the area of bridge pier: three-dimensional rendering in MeshLab software system (own elaboration) for measurement series no 4

Table 4 summarizes the results of the afflux calculations according to the Rehbock (Eq. (2.2)) and Yarnell (Eq. (2.3)) formulas, represented by  $\alpha_o$  – the measure of the contraction and  $\omega$  – the ratio of the velocity head to the water depth in the cross-section downstream the bridge. Table 4 also provides the results of calculating headwater afflux height  $\Delta h$  upstream of the bridge pier using the optimized Rehbock equation (Eq. (3.1)) and Yarnell equation (Eq. (3.2)). The measure of data matching was the relative error value  $\delta_s$  of the calculated afflux relative to the measured afflux height. The following forms of optimized functions were generated:

Table 3. Hydraulic parameters of laboratory experimental series summary table

No.	$Q_w$ [m <sup>3</sup> ·s <sup>-1</sup> ]	$h_0$ [m]	$q$ [m <sup>3</sup> ·s <sup>-1</sup> ·m <sup>-1</sup> ]	Fr [-]	$v_1$ [m·s <sup>-1</sup> ]	$v_3$ [m·s <sup>-1</sup> ]	$I$ ·10 <sup>-3</sup> [-]	$\Delta h_M$ [m]
1	0.0304	0.1201	0.052	0.45	0.436	0.473	5.0	0.0094
2	0.0401	0.1411	0.069	0.48	0.490	0.540	6.8	0.0130
3	0.0398	0.0900	0.069	0.97	0.762	0.858	0.9	0.0100
4	0.0399	0.1205	0.069	0.68	0.571	0.676	7.6	0.0187
5	0.0350	0.1400	0.060	0.41	0.431	0.465	5.7	0.0103
6	0.0351	0.1006	0.061	0.82	0.602	0.734	5.5	0.0181
7	0.0301	0.1011	0.052	0.68	0.513	0.616	6.9	0.0168
8	0.0300	0.1433	0.052	0.32	0.361	0.373	2.7	0.0045
9	0.0350	0.1200	0.060	0.56	0.503	0.570	6.7	0.0141
10	0.0400	0.1019	0.069	0.90	0.677	0.816	3.8	0.0174
11	0.0350	0.1150	0.060	0.60	0.525	0.597	6.3	0.0140
12	0.0300	0.1207	0.052	0.46	0.429	0.476	6.4	0.0120
13	0.0300	0.0970	0.052	0.70	0.533	0.631	5.8	0.0150
14	0.0305	0.1150	0.053	0.52	0.457	0.521	7.0	0.0140
15	0.0300	0.1150	0.052	0.51	0.450	0.509	6.8	0.0134
16	0.0300	0.1150	0.052	0.49	0.450	0.498	5.7	0.0111
17	0.0300	0.1150	0.052	0.50	0.450	0.504	6.3	0.0124
18	0.0350	0.1006	0.060	0.78	0.600	0.713	5.1	0.0160
19	0.0350	0.1200	0.060	0.57	0.503	0.575	7.1	0.0150
min	0.0300	0.0900	0.0517	0.32	0.3610	0.373	0.9	0.0045
max	0.0401	0.1433	0.0691	0.97	0.7625	0.858	7.6	0.0187

Where:  $Q_w$  – water discharge;  $h_0$  – water depth in a control profile;  $q$  – unit water discharge; Fr – Froude number;  $v_1, v_3$  – average stream velocity upstream and downstream the structure;  $I$  – energy gradient;  $\Delta h_M$  – measured afflux height.

– the optimized Rehbock formula (Eq. (3.1));  $a = 1.08, b = 1.79; c = 46.63$

$$(3.1) \quad \Delta h = \delta(1.08 + 1.79\alpha_0 + 46.63\alpha_0^4) (1 + 2\omega) \alpha_0 \frac{v_3^2}{2g}$$

– the optimized Yarnell formula (Eq. (3.2));  $d = 1.00, k = 15.00$

$$(3.2) \quad \Delta h = 2K(K + 10\omega - 0.6)(1.0\alpha_0 + 15\alpha_0^4) \frac{v_3^2}{2g}$$

Table 4. Original (2.2), (2.3) and optimised (3.1), (3.2) and (3.3), (3.4) formulas calculation results summary table

No.	$\alpha_0$ [-]	$\omega$ [-]	Eq. (2.2) $a = 0.72$ $b = 1.20$ $c = 40.00$		Eq. (3.1) $a = 1.08$ $b = 1.79$ $c = 46.63$		Eq. (2.3); (3.2) $d = 1.00$ $k = 15.00$		Eq. (3.3) $a = 1.08$ $b = 1.79$ $c = 46.63$		Eq. (3.4) $d = 1.00$ $k = 15.00$	
			$\Delta h_{RO}$ [m]	$\delta_s$ [%]	$\Delta h_{ROp}$ [m]	$\delta_s$ [%]	$\Delta h_{YO}$ $= \Delta h_{Yop}$ [m]	$\delta_s$ [%]	$\Delta h_{Rfr}$ [m]	$\delta_s$ [%]	$\Delta h_{Yfr}$ [m]	$\delta_s$ [%]
1	0.094	0.11	0.0018	80.7	0.0027	71.2	0.0036	61.7	0.0060	36.1	0.0080	15.0
2	0.095	0.13	0.0025	80.8	0.0037	71.8	0.0054	60.2	0.0096	26.5	0.0135	3.9
3	0.097	0.52	0.0102	2.4	0.0153	53.3	0.0434	334.0	0.0014	85.9	0.0040	60.0
4	0.102	0.26	0.0051	72.9	0.0076	60.1	0.0154	19.7	0.0115	38.7	0.0231	23.4
5	0.093	0.09	0.0017	83.7	0.0025	75.6	0.0030	70.6	0.0076	26.6	0.0091	11.7
6	0.105	0.37	0.0072	60.3	0.0108	42.0	0.0262	39.8	0.0083	54.1	0.0200	10.7
7	0.104	0.26	0.0044	73.9	0.0066	62.5	0.0135	24.6	0.0090	46.1	0.0182	8.3
8	0.089	0.06	0.0010	77.5	0.0015	68.1	0.0015	70.0	0.0033	25.6	0.0031	30.0
9	0.098	0.17	0.0030	78.6	0.0045	68.0	0.0075	47.0	0.0089	36.7	0.0148	4.7
10	0.104	0.47	0.0101	41.8	0.0152	19.8	0.0410	110.9	0.0063	63.5	0.0167	4.0
11	0.098	0.20	0.0035	75.3	0.0052	63.0	0.0092	33.9	0.0084	40.1	0.0150	6.8
12	0.096	0.12	0.0019	84.0	0.0029	76.5	0.0039	68.3	0.0078	35.0	0.0105	12.4
13	0.102	0.27	0.0045	70.3	0.0067	55.5	0.0140	6.7	0.0075	50.2	0.0157	4.4
14	0.098	0.15	0.0024	82.5	0.0037	73.8	0.0056	59.7	0.0087	37.7	0.0134	4.1
15	0.098	0.14	0.0023	82.8	0.0034	74.3	0.0052	61.5	0.0084	37.7	0.0125	6.6
16	0.095	0.13	0.0021	81.0	0.0032	71.5	0.0046	58.7	0.0068	38.4	0.0099	10.7
17	0.097	0.14	0.0022	82.1	0.0033	73.2	0.0049	60.5	0.0077	38.0	0.0114	8.4
18	0.103	0.34	0.0064	60.1	0.0095	41.8	0.0224	35.5	0.0074	53.7	0.0172	7.8
19	0.099	0.18	0.0031	79.2	0.0047	68.9	0.0078	47.9	0.0095	36.4	0.0160	6.5
	average		$\bar{\delta}_s$	71.6		62.7		66.9		42.6		12.9

Where:  $a, b, c$  – Rehbock formula (Eqs. (2.2), (3.1), (3.3)) dimensionless coefficients;  $d, k$  – Yarnell formula (Eqs. (2.3), (3.2), (3.4)), dimensionless coefficients;  $\alpha_0$  – the measure of the contraction;  $\omega$  – the ratio of the energy height upstream the structure to water depth downstream;  $\Delta h$  – the headwater afflux calculation result:  $\Delta h_{RO}$  – using the original Rehbock equation (2.2);  $\Delta h_{ROp}$  – using the optimized Rehbock equation (3.1);  $\Delta h_{YO}$  – using the original Yarnell equation (2.3);  $\Delta h_{Yop}$  – using the optimized Yarnell equation (3.2);  $\Delta h_{Rfr}$  – using the optimized modified Rehbock formula including the friction velocity;  $\Delta h_{Yfr}$  – using the optimized modified Yarnell formula including the friction velocity;  $\delta_s$  – the relative error of calculations.

As indicated by the calculations (Table 4), the Yarnell formula provided the best match of the original form of the function with the coefficients proposed in the original approach. The empirical formulas including friction velocity  $v_*$  introduction into original equations of Rehbock (Eq. (2.11)) and Yarnell (Eq. (2.12)) were then verified and optimized. To estimate friction velocity value, calculations of the hydraulic radius related to the bottom  $R_{hb}$  were performed according to the procedure described by Einstein (1950) [17] (Eq. (2.5)–(2.9)). A summary of the results is given in Table 4. Thus, the following optimized function forms were generated:

– the optimized Rehbock formula including the friction velocity

$$(3.3) \quad \Delta h = \delta(1.08 + 1.79\alpha_0 + 46.63\alpha_0^4) (1 + 2\omega) \alpha_0 \frac{(10v_*)^2}{2g}$$

– the optimized Yarnell formula including the friction velocity

$$(3.4) \quad \Delta h = 2K(K + 10\omega - 0.6)(1.00\alpha_0 + 15\alpha_0^4) \frac{(10v_*)^2}{2g}$$

It should be noted that the parameters of the optimized function (Eq. (3.4)) are the same as for the original formula (Eq. (2.3)).

## 4. Conclusions

Original Rehbock's formula (Eq. (2.2)) gave a fit described by an average relative error of 71.6% between headwater afflux estimation and measurement. The implementation of optimization techniques further reduced the average relative error to 62.7%. Therefore, an optimized formula that better describes the observed phenomenon was achieved.

For the original form of the Yarnell formula (Eq. (2.3)), a relative error of 66.9% was obtained. The optimization procedure demonstrated that in the studied range of coefficients variation, the original values of the parameters best describe the laboratory measurement results. The original formula is therefore the optimal formula, as confirmed by the bootstrap resampling procedure.

The research approach of velocity distribution areas downstream the bridge according to Einstein's assumption is proven to be appropriate, considering the low and the very low average relative error obtained for the calculations using the modified Rehbock formula (Eq. (3.3)) of 42.6% and for Yarnell formula (Eq. (3.4)) of only 12.9%.

The relatively close results of calculations and measurement may contribute to setting a new direction of engineering research, including friction velocity contribution in headwater afflux investigations. However, it should be emphasized that the research was conducted for laboratory, model conditions, which cannot be directly transferred to real objects because of the scale effect, therefore to conclude on the validity of formula coefficients change, it would be necessary to verify the optimized form of formulas on real objects with different dimensions, channel shape, and granulation conditions. Moreover,

results concern the three-column pillar without junction wall case and extending their range of applicability would demand additional research.

Most laboratory flumes, but also natural rivers, have enough hydrological and geometrical data to perform calculations using empirical equations. These equations, optimized by various methods, among which bootstrap resampling is proposed for engineering practice, can therefore allow relatively fast estimation of headwater afflux and can be used at the pre-design stage, where no very high precision results are required.

## Acknowledgements

The article was developed as a result of a research project no. 2020/04/X/ST8/01504 financed by the National Science Centre, Poland.

## References

- [1] P.A. Johnson and D.A. Dock, “Probabilistic bridge scour estimates”, *Journal of Hydraulic Engineering*, vol. 124, no. 7, pp. 750–754, 1998, DOI: [10.1061/\(ASCE\)0733-9429\(1998\)124:7\(750\)](https://doi.org/10.1061/(ASCE)0733-9429(1998)124:7(750)).
- [2] S. Naprawa, “Modeling deterioration and degradation of water headworks infrastructure assets”, *Acta Scientiarum Polonorum Architectura*, vol. 16, no. 3, pp. 81–87, 2017, DOI: [10.22630/ASPA.2017.16.3.08](https://doi.org/10.22630/ASPA.2017.16.3.08).
- [3] Ł. Krysiak, “The impact of riverbed erosion on the technical condition of water engineering structures: The example of Vistula river reach near the outlet of Wilanówka stream”, *Acta Scientiarum Polonorum Architectura*, vol. 17, no. 4, pp. 71–81, 2018, DOI: [10.22630/ASPA.2018.17.4.42](https://doi.org/10.22630/ASPA.2018.17.4.42).
- [4] W.H. Graf, *Fluvial hydraulics*. Chichester: John Wiley and Sons Ltd., 1998.
- [5] Q. Xiang, et al., “Experimental study of local scour around caissons under unidirectional and tidal currents”, *Water*, vol. 12, no. 3, art. no. 640, 2020, DOI: [10.3390/w12030640](https://doi.org/10.3390/w12030640).
- [6] S.H. Ju, “Determination of scoured bridge natural frequencies with soil–structure interaction”, *Soil Dynamics and Earthquake Engineering*, vol. 55, pp. 247–254, 2013, DOI: [10.1016/j.soildyn.2013.09.015](https://doi.org/10.1016/j.soildyn.2013.09.015).
- [7] M. Kiraga, J. Urbański, and S. Bajkowski, “Adaptation of selected formulas for local scour maximum depth at bridge piers region in laboratory conditions”, *Water*, vol. 12, no. 10, art. no. 2663, 2020, DOI: [10.3390/w12102663](https://doi.org/10.3390/w12102663).
- [8] G. Seckin, et al., “Bridge afflux estimation using artificial intelligence systems”, *Proceedings of the Institution of Civil Engineers – Water Management*, vol. 164, no. 6, pp. 283–293, 2011, DOI: [10.1680/wama.2011.164.6.283](https://doi.org/10.1680/wama.2011.164.6.283).
- [9] Z. He, et al., “Research of optimal experiment on bridge pier types for reducing headwater”, *MATEC Web of Conferences*, vol. 25, art. no. 04001, 2015, DOI: [10.1051/mateconf/20152504001](https://doi.org/10.1051/mateconf/20152504001).
- [10] R. Lamb, et al., “Recent advances in modelling flood water levels at bridges and culverts”, in *RandD Technical Report W5A-061/TR1*. 2006.
- [11] B. Liang, et al., “Local scour for vertical piles in steady currents: review of mechanisms, influencing factors and empirical equations”, *Journal of Marine Science and Engineering*, vol. 8, no. 1, art. no. 4, 2020, DOI: [10.3390/jmse8010004](https://doi.org/10.3390/jmse8010004).
- [12] T. Rehbock, “Zur Frage des Bruckenstanes”, *Zentralblatt des Bauverwattung*, vol. 39, no. 37, pp. 341–347, 1919.
- [13] D.L. Yarnell, “Bridge piers as channel obstruction”, *U.S. Dept. of Agriculture, Technical Bulletin*, pp. 442–451, 1934.
- [14] J. Kubrak and E. Nachlik, *Hydrauliczne podstawy obliczania przepustowości koryt rzecznych*. Warsaw: Wydawnictwo SGGW, 2003.
- [15] T. Tymiński, “Hydraulic model research on bridge piers based on the example of selected bridges in Opole”, *Annual Set the Environment Protection*, vol. 12, no. 51, pp. 879–893, 2010.

- [16] H.A. Einstein, “The bed load function for sediment transportation in open channels”, *Technical Bulletin*, no. 1026, 1950.
- [17] J. Urbański, “Influence of flow conditions in weir model on depth of local scour”, *Scientific Review Engineering and Environmental Sciences*, vol. 18, no. 2, pp. 21–29, 2009.
- [18] L.C. Van Rijn, *Principles of Sediment Transport in Rivers, Estuaries and Coastal Seas*. Amsterdam: Aqua Publications, 1993.
- [19] G. Bollrich and G. Preißler, *Hydromechanik, Band 1*. Berlin: Verlag für Bauwesen, 1992.
- [20] J. Szelka and Z. Wrona, “The employment of intelligent databases in bridge construction”, *Acta Scientiarum Polonorum Architectura*, vol. 16, no. 3, pp. 129–135, 2017, DOI: [10.22630/ASPA.2017.16.3.13](https://doi.org/10.22630/ASPA.2017.16.3.13).
- [21] H. Bałuch and I. Nowosińska, “Application of artificial neural networks in planning track superstructure repairs”, *Archives of Civil Engineering*, vol. 66, no. 4, pp. 45–60, 2020, DOI: [10.24425/ace.2020.135208](https://doi.org/10.24425/ace.2020.135208).
- [22] B. Mielczarek, “Sampling methods in Monte Carlo simulations”, *Prace Naukowe Instytutu Organizacji i Zarządzania*, vol. 25, no. 83, pp. 187–199, 2007.
- [23] J.E. Gentle, *Random number generation and Monte Carlo methods*. New York: Springer-Verlag, 1998.

## Szacowanie spiętrzenia powyżej mostu z wykorzystaniem metody bootstrap resampling

**Słowa kluczowe:** budowle wodne, budownictwo mostowe, gospodarka wodna, lokalne rozmycie, rumowisko, wezbranie

### Streszczenie:

Zabudowanie koryta rzeki filarami i przyczółkami mostu powoduje zwężenie jego przekroju. Wpływa to zmiany warunków przepływu, które widoczne są przede wszystkim podczas wezbrań katastrofalnych. Następuje wtedy zwiększenie prędkości przepływu oraz spiętrzenie wody przed mostem. Zmiany te zależą od geometrii koryta cieką oraz przekroju mostowego, a szczególnie stopnia zwężenia strumienia pod mostem. Warunki hydrauliczne pod mostem zależą od prędkości przepływu, wymiarów i kształtu podpór, składu granulometrycznego rumowiska, które scharakteryzować można ilościowo za pomocą współczynników oporów hydraulicznych. Tematyka badawcza spiętrzenia pod mostem stawiana jest na równi z rozpoznaniem procesów morfodynamicznych zachodzących na długości przeprawy. Spiętrzenie pod mostami określa się wzorami empirycznymi oraz metodą energetyczną wykorzystującą prawo Bernoulliego. Metody empiryczne optymalizuje się przyjmując różne kryteria statystyczne.

W celu opracowania strategii przeciwpowodziowej poziomy zwierciadła wody w okolicach budowli wodnych powinny być kontrolowane, obserwowane lub szacowane z modelowania przepływu wód wezbraniowych [8]. Spadki podłużne zwierciadła wody na długości koryt rzecznych zależy od warunków przegrodzenia cieką oraz od lokalnych warunków granulometrycznych wyznaczających opory hydrauliczne przepływu. Opory przepływu są charakteryzowane za pomocą współczynników empirycznych lub naprężeń stycznych na obwodzie zwężonym koryta cieką, wyrażanych według wartości prędkości dynamicznej.

Badania lokalnego piętżenia wody zostały zapoczątkowane pod koniec XIX wieku przez D’Aubuissona, którego formuła do szacowania wielkości afflux w oparciu o warunki hydrauliczne była weryfikowana przez Weisbacha i in. 1848 i Rühlmanna i in. 1880 [9]. Na początku XX wieku Naglar i Lane za pomocą własnych danych eksperymentalnych zweryfikowali formułę D’Aubuissona i zmodyfikowali formułę Weisbacha [9]. Następnie Rehbock i Yarnell przeprowadzili dużą liczbę eksperymentów laboratoryjnych, kontynuując tym samym wcześniejsze badania spiętrzenia mostowego.



W praktycznym użyciu pozostaje zaledwie kilka formuł, pozwalających na szacowanie spiętrzenia powyżej filarów mostowych. Poza formułami Rehbocka, Yarnella, Naglera i D'Aubuissona używa się formuły USBR. Niewielka liczba podejść badawczych i eksperymentów skupionych na badaniu zjawiska spiętrzenia pod mostami wskazuje, że weryfikacja wyników jest trudna z uwagi na lokalny zasięg danych i opracowań [10]. Rozpatrywaniu zjawiska rozmywania dna powinno towarzyszyć poznanie warunków formowania się lokalnych spiętrzeń. Liang i in. [11] przytaczają 30 eksperymentów różnych autorów, których efektem było uzyskanie formuły do oszacowania geometrycznych parametrów lokalnych rozmyć, a formuły do określenia wielkości spiętrzenia w użyciu jest zaledwie 10 [10].

Zastosowanie wielu metod obliczeniowych dostarcza rozbieżności uzyskiwanych wyników. Biorze się to z faktu, że metody obliczeniowe były weryfikowane tylko dla określonych warunków hydraulicznych (przepływy, geometria rzeki). Oszacowanie niepewności uzyskanych wartości to ważne elementy analizy hydraulicznej. Niezależnie od doboru właściwej formuły do szacowania spiętrzenia pod mostem, problemem badawczym pozostaje uzyskanie wiarygodnych danych do ich walidacji. W warunkach przepływów niskich spiętrzenie pod mostem jest praktycznie niezauważalne – staje się obserwowalne dopiero w warunkach przepływów wezbraniowych. W okresach tych jednak prowadzenie pomiarów jest niebezpieczne, a czasami niemożliwe. Wpływ mostów na poziom wód powodziowych powinien być rozpoznany dla celów planowania, projektowania, modelowania hydraulicznego, analizy ryzyka, jak również utrzymania i zarządzania w warunkach incydentów i katastrof powodziowych.

W artykule porównano spiętrzenie pod mostem obliczone za pomocą dwóch znanych formuł empirycznych Rehbocka oraz Yarnella i porównano je z wynikami badań laboratoryjnych. Kierując się przesłanką, że na ukształtowanie swobodnego zwierciadła wody w rejonie mostu wpływają także opory przepływu, podjęto próbę włączenia prędkości dynamicznej do formuł empirycznych. Na podstawie własnej bazy danych współczynniki wykorzystanych formuł zoptymalizowano z użyciem metody bootstrap resampling w symulacji Monte Carlo.

Przeprowadzone analizy wykazały, że formułą najlepiej opisującą zjawisko spiętrzenia pod mostem jest formuła empiryczna zbudowana na podstawie historycznej formuły Yarnella. Uwzględniając w niej prędkość dynamiczną i optymalizując uzyskano średni błąd względny 12.9%. Taka wartość średniego błędu względnego potwierdza słuszność przyjętego podziału pola prędkości na odpływie. Stwierdzono, że metoda bootstrap resampling w symulacji Monte Carlo stanowi użyteczne narzędzie inżynierskie przy optymalizacji formuł w badaniach hydraulicznych. Szczególnie cennym elementem artykułu jest wykorzystywanie próby danych historycznych.